Journal of Structural Geology 32 (2010) 1257–1270

Contents lists available at ScienceDirect

Journal of Structural Geology

journal homepage: www.elsevier.com/locate/jsg

Why joints are more abundant than faults. A conceptual model to estimate their ratio in layered carbonate rocks

Riccardo Caputo

Department of Earth Sciences, University of Ferrara, via Saragat 1, 44100 Ferrara, Italy

ARTICLE INFO

Article history:
Received 29 January 2008
Received in revised form
5 May 2009
Accepted 20 May 2009
Available online 6 June 2009

Keywords:
Fractures
Brittle deformation
Rock mechanics
Stress variability

ABSTRACT

It is a commonplace field observation that extension fractures are more abundant than shear fractures. The questions of how much more abundant, and why, are posed in this paper and qualitative estimates of their ratio within a rock volume are made on the basis of field observations and mechanical considerations. A conceptual model is also proposed to explain the common range of ratios between extension and shear fractures, here called the *j*/*f* ratio. The model considers three major genetic stress components originated from overburden, pore-fluid pressure and tectonics and assumes that some of the remote genetic stress components vary with time (*i.e.* stress-rates are included). Other important assumptions of the numerical model are that: i) the strength of the sub-volumes is randomly attributed following a Weibull probabilistic distribution, ii) all fractures heal after a given time, thus simulating the cementation process, and therefore iii) both extensional jointing and shear fracturing could be recurrent events within the same sub-volume. As a direct consequence of these assumptions, the stress tensor at any point varies continuously in time and these variations are caused by both remote stresses and local stress drops associated with *in-situ* and neighbouring fracturing events. The conceptual model is implemented in a computer program to simulate layered carbonate rock bodies undergoing brittle deformation. The numerical results are obtained by varying the principal parameters, like depth (*viz.* confining pressure), tensile strength, pore-fluid pressure and shape of the Weibull distribution function, in a wide range of values, therefore simulating a broad spectrum of possible mechanical and lithological conditions. The quantitative estimates of the *j*/*f* ratio confirm the general predominance of extensional failure events during brittle deformation in shallow crustal rocks and provide useful insights for better understanding the role played by the different parameters. For example, as a general trend it is observed that the *j*/*f* ratio is inversely proportional to depth (*viz.* confining pressure) and directly proportional to pore-fluid pressure, while the stronger is the rock, the wider is the range of depths showing a finite value of the *j*/*f* ratio and in general the deeper are the conditions where extension fractures can form. Moreover, the wider is the strength variability of rocks (*i.e.* the lower is the *m* parameter of the Weibull probabilistic distribution function), the wider is the depth range where both fractures can form providing a finite value of the *j*/*f* ratio. Natural case studies from different geological and tectonic settings are also used to test the conceptual model and the numerical results showing a good agreement between measured and predicted *j*/*f* ratios.

1. Introduction

Extension fractures, represented by joints and veins (the latter being mineral-filled joints), appear to be much more abundant than faults. The proportion between the two brittle deformational features mainly depends on the tectonic setting, but in weakly deformed sedimentary terrains, the ratio between the number of extension fractures and the number of faults (here called the *j*/*f* ratio) is always very high. Why is this?

Since this note will focus on brittle tectonic structures as commonly observed by a geologist in the field at the meso-scale, an introduction is provided to the terminology used in this paper. From a mechanical point of view, any interruption of the otherwise continuous properties of a rock mass is a *discontinuity*. Any discontinuity caused by any stress field is a *fracture* irrespective of its scale. This distinction is necessary in order to separate, for example, bedding planes from fractures. Any stress field potentially generating a fracture can be visualised by a unique stress tensor

E-mail address: rcaputo@unife.it

0191-8141/$ – see front matter © 2009 Elsevier Ltd. All rights reserved.
doi:10.1016/j.jsg.2009.05.011

virtually composed of different genetic components (Caputo, 2005) as discussed in a later section.

At the grain scale all fractures involve displacement, either dilation or shear or a combination of the two, though at the scale of observation possible in the field it may not be straightforward to measure the magnitude of the displacement if it is much less than about 1 mm (see discussions in Hancock, 1985; Pollard and Aydin, 1988; Dunne and Hancock, 1994). In this paper, fractures are classified according to the displacement vector, which connects two points contiguous before failure. This vector is partitioned in a component tangential to the fracture plane and a normal one. The ratio between the two or the angle between the displacement vector and the normal to the fracture plane can be a simple and objective parameter to express the type of displacement that occurred and therefore to classify a fracture. Accordingly, if the former component is predominant, we refer to a *fault*, if the opposite is true to an *extension joint*, while the intermediate cases are commonly referred to as *hybrid fractures* (Hancock, 1985; Price and Cosgrove, 1990).

In principle, fractures can show all possible values between 'ideal' extension joints ($\alpha = 0^\circ$) and 'ideal' faults ($\alpha = 90^\circ$), but based on more than 20 years of field observations, fractures with an oblique displacement ($\sim 10^\circ < \alpha < \sim 85^\circ$) are the rarest. Also on a theoretical ground, based on a critical review of i) the theoretical aspects of mixed mode ruptures (Lawn, 1993), ii) the results of laboratory experiments and iii) field case studies, Engelder (1999) argued that the transitional-tensile rupture process, which produces planar hybrid fractures, is unlikely to occur in homogeneous isotropic rocks, though it is possible in particular cases of inhomogeneous anisotropic materials.

Accordingly, as far as the competition between extensional and shearing fracturing events is here considered from a statistical point of view by analysing large numbers of fractures, hybrid features will be neglected in the following discussion and the associated conceptual model. A mineral-filled fracture is commonly referred to as a *vein*. For the sake of simplicity, in the following we will simply refer to joints and faults, respectively as extensional and shear fractures, irrespective of the occurrence of healing material whose role is further discussed in a later section.

The principal aims of this note are i) to suggest possible causes that facilitate the formation of joints instead of faults, ii) to propose a conceptual model to investigate the evolution of a carbonate rock mass, which frequently represents important reservoirs for water and hydrocarbons, during a distinctive brittle deformational event, considering both extension and shear fractures to be geologically coeval and iii) to understand the role played by the most important mechanical and geological parameters. For the latter aim, numerous computer simulations are performed based on a wide range of values of the input parameters.

Although the proposed conceptual and numerical models have been specifically applied to, and tested with, carbonate rocks, showing a good fit between the *j*/*f* ratio measured in several natural case studies and the numerically predicted values, the general results can be certainly exported to other layered lithologies provided that the proper mechanical parameters are considered.

2. Mechanical aspects of the elastic–brittle behaviour

2.1. Qualitative approach

All laboratory tests on rock samples show that the absolute value of the tensile strength, T_0, is lower than the compressive strength, C_0 (*e.g.* Brace, 1964; Jaeger and Hoskins, 1966). The experimental ratio between C_0 and T_0 is usually much more than 10 (*e.g.* Brace, 1964), which is also in agreement with the value predicted by the extended Griffith theory (Murrell, 1963) and comparable to that obtained from the modified Griffith theory (see Jaeger and Cook, 1979). In other terms, a negative stress-rate (tensile conditions) will produce extensional fractures more easily (*i.e.* lower involved energy) than a similar, but positive stress-rate (compressive conditions). A common example is provided by a beam during a folding process. Indeed, in the fold hinge a fibre stress symmetrically develops departing from the neutral surface (Chapple, 1969; Price and Cosgrove, 1990), being tensile and compressive in the outer and inner arcs, respectively. If the folded material has an elastic–brittle behaviour, with increasing buckling the beam will always fail in the outer arc under tensile conditions forming an extensional fracture, but never in the inner arc.

Secondly, an important difference between the mechanical parameters when estimated from tensile *versus* compressive tests, is the Young's modulus (Fairhurst, 1961). For rocks, its value is generally less under tension than under compression (*i.e.* $E_T < E_C$). This implies that the application of equal values of loading, but opposite in sign, will produce larger strains (as absolute values) in tension than in compression. This phenomenon is interpreted as due to the occurrence of Griffith cracks within all natural materials that can open more easily under tension than closing under compression, thus decreasing in the former case the overall strength of the rock at the sample- or meso-scale. For example, loading conditions producing equal amounts of linear stress but opposite in sign will generate absolute values of the linear strain greater in extension (lengthening in this case) than in contraction (*viz.* shortening). Accordingly, the higher the strain, the more important or more numerous are the deformational structures required to accommodate it. Once again, tensile fractures will be statistically more represented than compressional ones (*i.e.* shearing events).

Thirdly, at shallow crustal levels (for example a few hundred metres), differential stresses are usually relatively low (Etheridge, 1983) and in many cases much lower than those required for shear fracturing (Jaeger and Cook, 1979). Accordingly, if differential stresses are low enough, critical conditions for failure as described, for example, by the Mohr's envelope can be reached more easily, or exclusively, in tensile conditions, therefore enhancing the inception and growth of extension joints within a rock volume rather than the faulting (*i.e.* shearing) process.

A final remark concerns the different finite strain accommodated by the two kinds of tectonic structures (joints and faults) in carbonate rocks undergoing light-to-moderate deformation. Indeed, the lengthening perpendicular to the fracture plane that a single extension joint can produce, which may be simply represented by the amount of opening, is commonly much smaller than the mean lengthening that even a small meso-scale fault can produce in the direction of the σ_3. Rare exceptions are represented by sedimentary and magmatic dykes. However, in the former case very shallow conditions and strong lateral topographic gradients are necessary, while the latter type occurs only in volcano–tectonic environments. Because both cases could be easily recognised in the field, it could be safely stated that, if a rock volume needs to accommodate a given amount of stretching, two end-members scenarios can occur, in which few conjugate faults are formed or alternatively numerous extension joints affect the entire mass. All the intermediate combinations are obviously possible, giving rise in any case to large joints to faults ratios.

2.2. Stress variability

In the presence of an opening component, fractures at diagenetic depth are generally healed by a contemporaneous crystalline cement (*e.g.* Laubach et al., 2004a; Gale et al., 2004), which in

carbonate rocks is usually sparite (*i.e.* sparry calcite). The healing of a newly formed fracture due to post-failure cementation is fundamental during brittle deformation of a rock mass because this diagenetic process may strongly influence the stress evolution within a broader rock volume hosting the vein. According to fracture mechanics theory, when extensional failure occurs, the surrounding stress field is highly perturbed. In particular, the tensile stress perpendicular to the fracture plane is strongly reduced and a new fracturing event is hampered within a distance of a few times the size of the joint (Ladeira and Price, 1981; Pollard and Segall, 1987). For example, in layered rocks, where joints commonly do not exceed the layer thickness, Pollard and Segall (1987) have calculated that, at a distance 1.5 times the joint length, the stress component normal to the fracture plane is 85% of the remote stress, while it reaches 99% only at a distance 6 times the bed thickness (*viz.* the joint length). This effect has been also claimed by Ladeira and Price (1981) to explain the regular spacing of joints in layered rocks (see also Harris et al., 1960; Price, 1966, p. 144; Bai and Pollard, 2000).

As a consequence, while a fracture is not healed, it represents a "free surface" where the normal principal stress is equal to the fluid pressure and a stress gradient exists departing from both sides of the fracture plane rising up to the "normal" remote stress value. In these conditions, the minimum spacing for the nearest parallel joint that can form in the meantime depends on the lateral extent of the perturbed stress field, which in turn is a direct function of the elastic properties of rocks, the joint size and the mechanical unit thickness (*e.g.* Hobbs, 1967; Ingraffea, 1987; Gross, 1993; Gillespie et al., 2001). However, once the fracture is completely healed, the physical and mechanical continuity is restored and local stresses can build up again according to the remote stress field, while critical strength conditions can be achieved once more thus generating a new failure event (Caputo, 1995). At this stage of the brittle process, two alternative mechanisms of jointing can occur. If the vein infilling (*viz.* cement) is weaker than the host rock, then the *crack-seal* mechanism occurs as described by Ramsay (1980) and the new failure usually follows a path along the rock–vein interface or across the vein material itself. By contrast, if the healing material is more resistant to tension than the surrounding rock, a new and independent fracture is initiated within previously intact rock. In the latter case, a *crack-jump* mechanism occurs (Caputo and Hancock, 1999), which is relatively common in carbonate rocks (*e.g.* Roberts, 1974; Rawnsley et al., 1998; Peacock, 2004; Caputo et al., 2008). On one hand, the prevalence of either mechanism strongly depends on the lithology of the host rock, because the tensile strength of sparry calcite could be considered as relatively uniform throughout a rock volume and even in different lithologies and geological settings. On the other hand, from a structural point of view, the predominance of one of the two above mentioned rupture mechanisms bears important consequences, especially at the outcrop scale. Indeed, in sedimentary rocks stretched parallel to bedding, if the crack-seal process prevails, individual beds will be crossed by relatively few and thick veins accumulating most of the lengthening, each one representing many failure events. If the opposite occurs, that is the crack-jump mechanism is more frequent, the effects of recurrent fracturing will pervade the entire layer, which will be affected by many hair-like, closely spaced extension veins.

The active jointing mechanism influences as well the final number of joints and hence the joints to faults ratio. Indeed, in carbonate rocks where the vein infilling consists of sparite, the amount of released elastic energy associated with the crack-jump mechanism is less than the amount associated with the crack-seal one, thus implying that the maximum opening will be smaller in the former case (Caputo and Hancock, 1999). Therefore, considering two carbonate layers, respectively softer and stronger than sparite, a larger number of crack-jump events than crack-seal events will be necessary to accommodate the same amount of bed-parallel stretching. As a consequence, the final number of extension fractures will strongly differ in the two cases.

Stress variability also occurs in triaxial stress conditions. Let us assume two horizontal remote tensile stresses, with an E–W oriented σ_3 and a N–S σ_2. When failure conditions are reached, a N–S vertical joint will form. Due to the stress drop occurring in the E–W direction and till the fracture remains open, the N–S principal stress locally becomes the σ_3, therefore producing a *stress swap* within a volume surrounding the joint (Caputo, 1995). If the remote stress continues to accumulate, failure conditions can be reached again, but a new extension joint will form perpendicular to the former one. This second failure event will thus generate a new stress swap. Numerical calculations based on this conceptual model (Caputo, 1995) have confirmed the local parallelism of the σ_3 axis with pre-existing systematic joints and estimated the stress conditions for the formation of orthogonal cross-joints (Bai et al., 2002). If the mechanism is repeated several times within a rock mass, a typical grid-lock fracture system will be produced (Hancock et al., 1987; Caputo, 1995). It consists of two roughly perpendicular joint sets showing mutual abutting relationships, with the fractures of one set that stop the propagation of the fractures of the other set, and vice versa. This documents that the two sets are geologically coeval and could be used in mesostructural analyses for numerical inversion of palaeostress fields (*e.g.* Caputo and Caputo, 1989; Caputo, 1991).

3. Conceptual model

Any stress field can be represented at any point by a unique stress tensor, **T**. However, stress fields originate from several sources, including thermal, overburden, pore-fluid, tectonic, anthropogenic and diagenetic processes, all independently pervading, with different magnitudes, rock volumes of different size. The stress tensor can thus be virtually visualised at any point as the sum of several tensors, each representing a different *genetic component* (Caputo, 2005):

$$\mathbf{T}_{\text{total}} = \mathbf{T}_{\text{gravity}} + \mathbf{T}_{\text{fluids}} + \mathbf{T}_{\text{tectonic}} + \mathbf{T}_{\text{thermal}} + \mathbf{T}_{\text{anthropogenic}} + \mathbf{T}_{\text{diagenetic}} + \cdots \quad (1)$$

For the specific goals of the proposed model, only few of these components will be briefly discussed. For a more exhaustive description and discussion also concerning the thermal and diagenetic components, see Caputo (2005). The importance of the gravitational component in any stress field is well known. Indeed, the pressure generated by the weight of the overburden is proportional to the burial depth and the integral density of the overlying rocks. Therefore, this genetic component always increases downwards. Moreover, laboratory experiments have demonstrated that several mechanical properties of the rocks depend on the confining pressure (*e.g.* Jaeger and Cook, 1979): consequently, the same rock can behave differently at different depths and, although experiencing comparable differential stresses, it will deform in different ways. On the other hand, if erosion or sedimentation occurs at the surface, this genetic component will vary with time, thus introducing a stress-rate in $\mathbf{T}_{\text{total}}$.

The permeability of rocks is also an important parameter to be considered. Permeability depends on the porosity of a rock and on the distribution and size of the interconnected pores and fractures.

In the uppermost crust it is almost always present. Thus, fluids pervade the rock mass and usually an internal pore-fluid pressure is exerted outwards. Its reference value at any depth is the hydrostatic pressure, but abnormally high fluid pressures are common at depths exceeding a few hundred metres in the crust (Fyfe et al., 1978; Fertl et al., 1994). In places, the ratio between pore-fluid pressure (p_f) and lithostatic pressure (p_c), commonly referred to as λ_e, approaches or exceeds 1. A number of processes have been suggested, among which the most common are i) a rapid compaction without leakage (*i.e.* compaction disequilibrium), ii) the injection of heated and expanding fluids (*i.e.* aqua-thermal pressuring), iii) hydrocarbon generation, iv) pressure solution and v) diagenetic dehydration reactions of minerals (Dickinson, 1953; Powers, 1967; Barker, 1972; Magara, 1975; Harrison and Summa, 1991; Renard et al., 1999; Tuncay et al., 2000). Even in rocks where such high λ_e values do not occur, extension fracturing and shearing are encouraged when fluid pressures exceed the minimum principal stress (σ_3). The role of fluid pressure in promoting the growth of fractures by reducing the inhibiting effect of confining pressure is also well known through the fundamental works of Terzaghi (1943) and Secor (1965). Also in this case, this genetic component can vary with time, due to continuing compaction or external fluid injection and, at the local scale, by the simple opening of fractures that can produce a pore-fluid pressure drop (*e.g.* Tuncay et al., 2000).

The tectonic component of the stress is the one most structural geologists pay attention to. From a genetic point of view, the tectonic component is basically induced by plate motion, which generates a first order stress field. At a smaller scale of observation, the tectonic component could be also associated with a second-, third- or even minor-order stress field induced by local conditions. A compressional stress field induced by continental convergence, a tensile stress field associated with the external bending of large-scale folds, or a strike-slip stress regime generated along a major transfer fault zone, are three possible examples of different tectonic genetic components occurring at different scales. Also in the time domain the tectonic genetic component can be quite constant or extremely variable, depending on the causative mechanism and the stress field hierarchy.

Sometimes one genetic component prevails over the others so that the stress field can be easily characterised. More often, however, the stress field is composite and the magnitude of each individual genetic contribution can be hardly separated. Each genetic component varies in space and time, with specific and different gradients and rates. This implies that the evolution of the total stress 250 tensor at any point in a rock mass can be very complex.

Another important issue is represented by the size of the rock volume within which a stress field can be considered more or less uniform. For example, stress trajectories are commonly smoothly curving at the scale of continents (*e.g.* Zoback and Zoback, 1991), while from rock mechanics it is well known that even a microscopic fracture strongly perturbs the local stress field (*e.g.* Jaeger and Cook, 1979; Atkinson, 1987). At an intermediate scale, structural geologists deal with outcrops with numerous meso-scale fractures, and they are often puzzled about which approach to follow.

4. Numerical model

4.1. Assumptions

The basic assumptions and the mathematical notations follow the work of Caputo (1995). In the present model, we consider a volume of rock at the outcrop scale, say in the order of 10^3 m^3, where remote forces generate a stress tensor with its principal components σ_x, σ_y and σ_z parallel to the E–W, N–S and vertical directions, respectively. As usual, σ_1, σ_2 and σ_3 correspond to the maximum, intermediate and minimum principal stress components, respectively. Regarding the sign of the value, the convention followed considers compressive and tensile stress, as positive and negative respectively.

When attempting to set up a numerical model of brittle deformation, a crucial point is to assume realistic values for the used parameters, and particularly for those concerning the remote stress field which governs the whole process. This exercise could be relatively simple in static conditions, but its complexity increases when stresses are function of time, as commonly happens in nature. In order to calculate realistic values and tentatively quantify the process at each time step of the numerical procedure, it is useful to analyse in detail some possible genetic component. At any given depth, the 'gravitative' component of the stress field, here considered as the confining pressure, p_c, is proportional to the mean density of the overlying rocks. Concerning the pore-fluid pressure, p_f, at shallow crustal conditions, say less than the 5 km here investigated, the value of p_f normally ranges between hydrostatic and lithostatic, that is to say $0.4 < \lambda_e < 1$ (*e.g.* Mouchet and Mitchell, 1989). However, in particularly shallow conditions up to few 100 m depth, rocks could be almost dry (*i.e.* $\lambda_e \sim 0$). Finally, a 'tectonic' genetic component generated by a stationary far-field regime is also assumed, which represents the real engine of the whole brittle deformational event.

When failure occurs, it is also assumed that all the components of the local stress tensor experience a significant drop in magnitude as a result of the sudden release of elastic energy. After the failure event, the same stress-rates that progressively 'charged' the rock mass reaching the failure conditions: i) continue to affect the local stress field as well as the whole rock mass; ii) generate continuous variations of the tensor components; and iii) will potentially restore the failure conditions. In summary, for the purpose of the model it is assumed that both extension and shear fracturing are recurrent processes and that all fractures are healed after a given lapse of time.

Averaged in space and time, the stress field acting on the deforming rock mass will mimic the far-field tectonic regime and any local stress release due to micro- or meso-scale fracturing will be always restored with time. As a first approximation, the rock mass remains in an average steady-state stress. The far-field tectonic stress attempts to restore itself anywhere and anytime following the local and temporal variation occurring due to fracturing. Consequently, brittle deformation can be regarded as being more or less uniformly distributed in space and time, though the assumption of a regular stress field characterised by smooth stress trajectories is not valid at a single point during time, nor for a given time in the whole volume (Caputo, 1995; Caputo and Hancock, 1999).

4.2. Analytical approach

It has been shown that, when modelling brittle deformation at the meso- and macro-scale, the use of a simplified approach based on Hooke's law and on the tensile or compressive strength of materials gives analytical solutions similar to those that can be obtained by applying a more refined Linear Elastic Fracture Mechanics, LEFM, approach (Caputo, 1995, 2001). There are a number of limitations in using the latter theory to describe the brittle behaviour of rock volumes at the outcrop scale. For example, in these conditions the LEFM principles are in direct conflict with the propagation of shear cracks (Ingraffea, 1987) and the propagation of meso-faults cannot be predicted using the LEFM shear-crack model (Engelder et al., 1993).

Problems also arise when one models the inelastic aspects of the deformation occurring around the crack-tip, because the LEFM theory only describes accurately the behaviour of cracks in case the size of the process zone is small compared with the length of the

fracture. The question of defining the mechanical conditions under which the LEFM can be reliably applied has been posed by Engelder et al. (1993). In order to by-pass such problems, the *tensile strength*, T_0, of rocks can be used instead of *stiffness*, especially in case of uniaxial tensile conditions. At this regard, a linear relationship between the two parameters has been documented for several rock types (Zhang, 2002; Al-Shayea, 2002). Given a mean value, the tensile strength is randomly assigned to the sub-volumes within the modelled rock mass (*i.e.* model's cells) following a Weibull probabilistic distribution (Weibull, 1939, 1951). This procedure takes into account that all rocks are characterised by lithological (*viz.* mechanical) heterogeneities as largely documented by laboratory tensile tests on identical materials and under the same mechanical conditions (Fig. 1).

In line with the above comments, the classical stress–strain relations (Jaeger and Cook, 1979) have been used and stresses have been calculated as the sum of different genetic components. Due to the above assumptions, and the consequent introduction in the model of stress-rates in one or more genetic components, stresses continuously vary in time and are re-calculated at each time step of the numerical procedure. Similarly, two critical failure conditions are checked at each time step; the Griffith criterion and the classical Coulomb criterion for jointing and shearing events, respectively.

In all cases, when failure conditions are reached, a fracture is virtually propagated. Assuming a layered rock characterised by weak bedding surfaces, the fracture dimensions will depend on the type of rupture process, either opening or shearing, and on the layer thickness. In particular, for joints, it is assumed that each propagation event is mechanically confined within a single layer, while faults cut through several layers. This difference reflects common field observations on outcrops of carbonate sedimentary rocks affected by brittle deformation (*e.g.* Peacock and Sanderson, 1991; Caputo, 1991; Peacock, 2002; Gillespie et al., 2001, among many others) as also clearly shown in the field examples discussed in a later section of the paper. Although the cumulative displacement associated with several in-plane rupture events could generate finite fracture planes with aspect (length/width) ratios ranging from 0.5 to 3.5 (*e.g.* Nicol et al., 1996), as a first approximation, the geometry of the rupture plane for both fracture types is assumed equidimensional. Tests with more complex fracture geometries do not show any significant influence on the results.

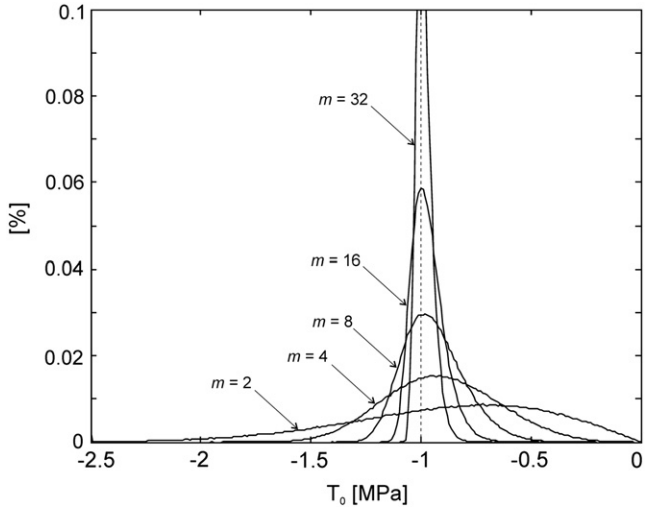

Fig. 1. Weibull statistical distributions of the tensile strength, T_0, used during the numerical simulations. The examples are obtained by fixing the mean tensile strength to −1.0 MPa and are based on different values of the shape parameter m (heterogeneity index) included in equation (2) (see text). The ordinate axis indicates the probability calculated for a bin size of 10 kPa. For the numerical simulations, the different Weibull distributions obtained by fixing different values of the mean T_0 and m are randomly assigned to the cells of the model. Note that the lower is the m value, the more the largest probability differs from the mean T_0 value (vertical dashed line).

Around the newly formed fracture a stress drop is imposed within a rock volume whose size is proportional to the structure dimensions (Caputo, 1995, 2005), being obviously smaller for a joint and larger for a fault. In particular, in the former case, the stress drop involves only the principal stress axis perpendicular to the rupture plane (σ_3), while in the latter case, the stress drop affects both maximum and minimum principal stress axes (σ_1 and σ_3). In the model, fractures are left open (*i.e.* as free surfaces) for a given number of time steps, thus simulating the time necessary for the cement precipitation to completely heal them.

As the remote stresses continue to act independently (*viz.* stress-rates are not nil), the local stress shadow (Nur, 1982) is progressively reduced in the sub-volumes of the model surrounding the fracture where stress drop occurred. Within the fractured cells, stresses can only build up again after the fracture is assumed to have been, at least partially, healed. If the stress-rate is very high and/or the cementation process too slow, this assumption may not be applicable. This aspect will be further discussed in a later section.

The simple probabilistic assumption that the rock strength of the model's unit cells follows a Weibull distribution, together with the use of mechanical criteria governing the rupture processes allows to reasonably combine the stochastic nature of the brittle deformational process with a deterministic approach, therefore providing more realistic simulations for large-scale volumes.

4.3. Numerical simulations

In order to simulate the brittle deformation occurring within a layered rock volume as observed at the outcrop scale, say a 10 m-sided cube with few decimetre-thick beds, the conceptual model above described has been applied to a cubic grid, consisting of $n \times n \times n$ cells, by implementing in-house software. The software follows the conceptual procedure discussed above and allows the number of fracturing events of the two types to be counted and hence their j/f ratio to be obtained. It is noteworthy that the model does not necessarily reproduce joints and faults as they are commonly observed and considered in the field by structural geologists. Indeed, within each cell of the model, which represents a sub-volume of a layer, it is not *a priori* predicted whether new critical failure conditions will produce a new distinct fracture plane or re-activate an older, previously healed one. The latter hypothesis is likely more common for shear planes, but for extension joints it depends on the prevailing mechanism within the rock mass, *i.e.* crack-jump (Caputo and Hancock, 1999) or crack-seal (Ramsay, 1980). Low tensile strength values of the rock mass will facilitate the former mechanism, therefore virtually producing a number of brittle structures more closely corresponding to the number of extensional failure events. This issue is further discussed in a subsequent section when comparing numerical results to observed field cases.

Firstly, numerous runs of the program have been carried out to test and optimise modelling parameters like total grid dimension, number of cells, cells size, boundary effects, total running time and the more convenient time step. A good compromise between the need of reducing the computing time and the stability of the obtained results is considered when the variation in the calculated j/f ratio induced by a further increase/decrease of a single parameter does not exceed a few percent. For example, by varying the product of the stress-rate by the time step of one order of magnitude no changes are observed in the j/f ratio. Similarly, as concerns the total running time, a stable j/f ratio is systematically reached after

a simulation of few tens of ka, therefore making feasible to reproduce deformational events of realistic length (ca. 10^5–10^6 years). Finally, regarding the number of cells and hence the total grid dimensions and cells size, it has been tested in the range 10^5–10^7 showing a fairly stable value of the calculated *j*/*f* ratio. In a second phase, the 'geological' and mechanical parameters have been systematically varied within assumed ranges to investigate their importance and their influence on the *j*/*f* ratio during brittle deformational events.

Depth has been varied from few tens of metres to some thousands of metres; the pore-fluid pressure was tested in the range $0 \leq \lambda_e \leq 0.9$, whereas the tensile strength was set between -0.1 and -15 MPa, which represent typical values for carbonate rocks from poorly consolidated calcarenites and calcilutites to stronger well cemented dolostones and limestones (Fookes and Higginbottom, 1975; Lama and Vutukuri, 1978; Jaeger and Cook, 1979; Carmichael, 1982; Christaras, 1997; Burton et al., 2001, 2003; Dinis da Gama and Navarro Torres, 2002; Austin and Kennedy, 2005; Karakus and Tutmez, 2006). In the mixed stochastic–deterministic approach here followed, another crucial parameter is represented by the *shape* of the Weibull probabilistic distribution function, *m*, also referred to as *homogeneous index*, used to randomly assign the tensile strength to the sub-volumes of the modelled rock mass

$$N = m \cdot \frac{T^{m-1}}{T_0^m} \exp^{\left[-(T/T_0)^m\right]} \quad (2)$$

where *N* is the probability that a cell bears a specific tensile strength (*T*) around a fixed mean value (T_0). In particular, the *shape* parameter (*m*) varied between 2 (*i.e.* large variability) and 32 (*i.e.* highly clustered values). Different probabilistic distributions of the tensile strength are shown in Fig. 1 based on a fixed mean value of -1 MPa and bin size of 10 kPa. During the numerical simulations, tensile strength values are attributed randomly to each cell of the model complying with Weibull probabilistic distribution functions and based on different values of the shape parameter.

Concerning the genetic components of the stress field, three in particular have been considered in this paper: for tectonics, a uniaxial tensile regime is imposed by considering negative stress-rates around 10^{-4} Pa s^{-1} in the σ_x direction. Based on common values of the Young modulus for carbonate rocks, these rates roughly correspond to realistic geological strain-rates of 10^{-13}–10^{-14} s^{-1}. As a first approach, for the confining pressure and the pore-fluid pressure (*i.e.* gravitative and fluid genetic components) a constant value is assumed, that is to say the occurrence of significant denudation or deposition during brittle deformation or fluid injection or depletion during fracturing has been considered negligible processes.

The assumptions of the numerical model are necessarily simplified, and are possibly not sufficient to reproduce in detail the complexity of real rock volumes during brittle deformation and consequently to obtain an 'exact' value of the *j*/*f* ratio. In spite of this, the several hundreds of numerical simulations carried out provide useful insights on the role played by the different parameters and interesting quantitative estimates on the expected *j*/*f* ratio in different geological settings. Accordingly, this 'predictive' approach could also represent a valuable tool for operators in the oil, water, waste management, mining and rock engineering industries, which commonly analyse a limited number of data (such as in poorly exposed areas or from drillings).

5. Results

The model parameters have been set to best simulate carbonate rocks characterised by a well defined layering that imposes a mechanical boundary for joints. This choice was also oriented to the selected field examples used for testing the model and for comparison with the numerical results (see later section).

From the several hundred numerical simulations, it is thus possible to infer the principal mechanical and geological parameters that play a major role during the fracturing process and that primarily influence the *j*/*f* ratio within a rock volume undergoing brittle deformation. In Figs. 2 and 3, the *j*/*f* ratio is represented as a function of depth. In particular, in Fig. 2, the curves represent different tensile strength values at a pore-fluid pressure (λ_e) that is constant for each diagram. In Fig. 3, for each diagram, the different curves represent different values of the pore-fluid pressure at constant mean tensile strength (T_0). Deeper conditions have been also tested confirming the general trends, but they are not represented in the figures.

5.1. Depth

The depth of the rock volume and hence the confining pressure is one of the most influencing parameters. As a general trend, the shallower the depth, the higher is the *j*/*f* ratio, which can vary over several orders of magnitude (Figs. 2 and 3). An interesting point emphasized by the numerical simulations is the existence of lower and upper thresholds. Below the lower threshold, critical stress conditions for producing faults are hampered because the differential stress is too low and local stresses are more easily released via extensional fracturing. In this case, the ratio tends to infinity. In contrast, toward the upper threshold, the opposite occurs and the local stress conditions for the creation of an extensional fracture progressively disappear, therefore reducing the number of joints and hence the *j*/*f* ratio to values lower than 1. The depth interval between the two thresholds, where the *j*/*f* ratio has a finite, value >1, varies between few 100 m and several kilometres, depending on the tensile strength and the pore-fluid pressure (see below).

5.2. Tensile strength

The tensile strength during a fracturing process plays an important role in determining the minimum and maximum depth at which faults and joints, respectively, can form. The more competent (*i.e.* stronger) is the rock mass, the wider is the range of depths at which both kinds of fractures can develop and hence the *j*/*f* ratio has a finite value. Moreover, the stronger the material, the deeper the maximum conditions where extension joints can form (Figs. 2 and 3). Within the tested interval of strength values (between -0.1 and -15 MPa), the maximum depth producing *j*/*f* ratios >1 shifts from few tens of metres to more than 5 km, with a hydrostatic pore-fluid pressure, and it is even deeper than 10 km with a highly supra-hydrostatic pore-fluid pressure.

5.3. Pore-fluid pressure

As expected, the general effect of the pore-fluid pressure is to enhance the tensile fracturing process by reducing the effective pressure. The results obtained from five sets of numerical tests are represented in Fig. 4a–e, where the tensile strength is kept constant for each diagram. The four curves in each graph consider a perfectly dry material (*i.e.* $\lambda_e = 0$), at hydrostatic pore-fluid pressure (*i.e.* $\lambda_e = 0.46$) and at supra-hydrostatic conditions ($\lambda_e = 0.7$ and $\lambda_e = 0.9$). The first one could represent very shallow conditions occurring in superficial deposits and rocks above the uppermost unconfined aquifer, while the latter simulate generally deeper conditions, for example where a rapid burial without a complete leakage has

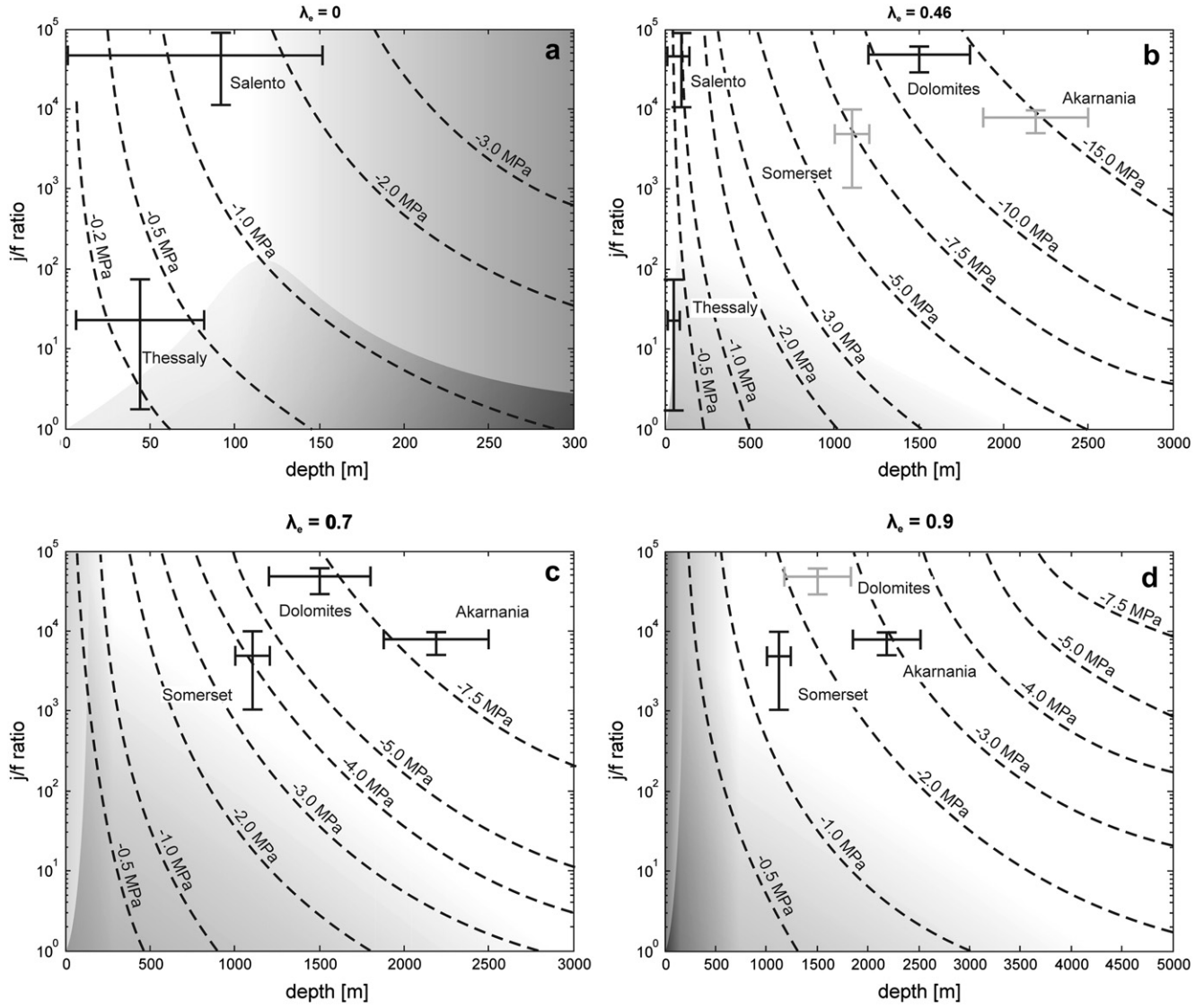

Fig. 2. Results of the numerical simulations based on the proposed conceptual model showing the *j*/*f* ratio as a function of depth (in metres). The different graphs represent different pore-fluid pressures: a) dry rocks ($\lambda_e = 0$); b) hydrostatic conditions ($\lambda_e = 0.46$); c) supra-hydrostatic conditions ($\lambda_e = 0.7$); d) highly supra-hydrostatic conditions ($\lambda_e = 0.9$). In each graph, the different curves represent different tested tensile strengths. Shaded areas indicate unlikely combinations of geological conditions. The curves crossing them are purely theoretical (see text for details and discussion on this issue). The *j*/*f* ratios measured in the field for the discussed case studies are plotted with the corresponding uncertainty bars showing an overall good agreement between predicted and measured values. Gray symbols indicate unlikely site conditions as constrained by one or more parameters.

occurred. In between, the intermediate λ_e value (=0.46) represents the common hydrostatic reference and it likely represents the most frequent geological conditions within the uppermost crustal levels.

Comparing the different conditions, the *j*/*f* ratio tends to increase with increasing pore-fluid pressure, and this also occurs for the depth interval of coexistence of both fracture types and for the maximum depth at which extension fractures can form. With sufficiently high pore–fluid pressure the model predicts favourable conditions for tensile fracturing even at depths of several kilometres, far beyond the commonly accepted conditions for extensional joints (*e.g.* Price and Cosgrove, 1990). However, these numerical results are in agreement with borehole data drilled in subhorizontal, poorly deformed carbonate rocks, therefore documenting the occurrence of open joints parallel to the present-day maximum horizontal stress at depths up to 6 km (Narr and Currie, 1982; Narr and Burruss, 1984; Laubach et al., 2004a). This behaviour probably depends on the reduced differential stress, a key parameter for the generation of faults.

5.4. Weibull parameters

As mentioned above, the strength of natural materials even for apparently similar lithologies is indeed quite variable at the sample scale (Curtis and Juszczyk, 1998; Davies, 2001). For many decades, it has been well documented that this variability follows a statistical distribution described by the Weibull probabilistic function (Weibull, 1939, 1951), where the degree of skewness and opening of the curve affects the heterogeneity distribution among sub-volumes, which could be relatively weaker or stronger than the fixed mean values (Fig. 1). Within a statistically significant rock volume, the larger the variability of strength values assumed for the model's cells (*viz.* lower *m*), the lower the depth interval where both kinds of fractures can form. In general, if compared with other rocks, limestones and dolostones show a very high strength variability (*e.g.* Al-Shayea, 2002; Backers, 2004; Liu et al., 2004; Chang et al., 2006).

In order to simulate the mechanical behaviour of a granite, which represents a natural material certainly more homogeneous

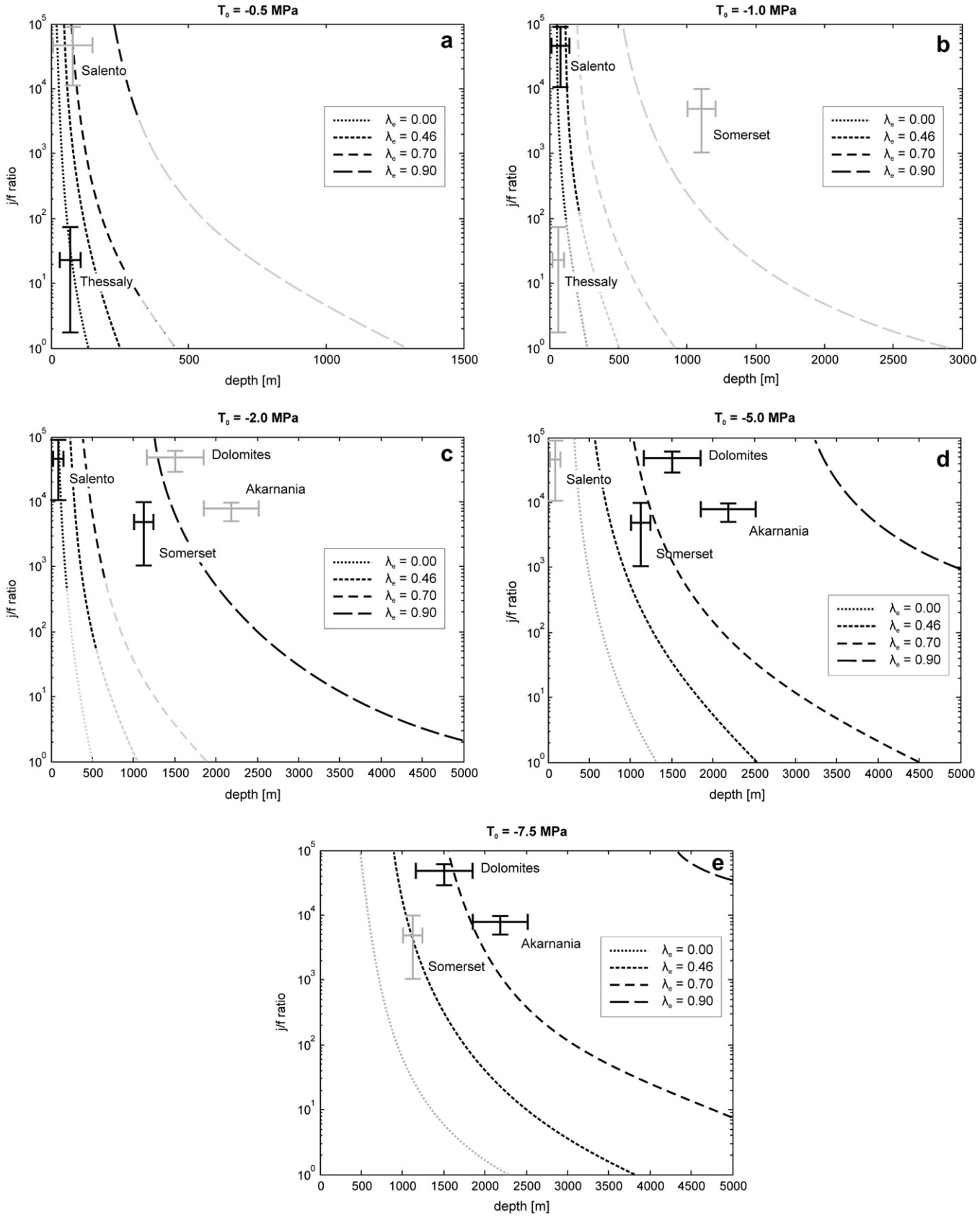

Fig. 3. Results of the numerical simulations based on the proposed conceptual model showing the *j*/*f* ratio as a function of depth (in metres). The different graphs represent different tensile strength values: a) −0.5 MPa; b) −1.0 MPa; c) −2.0 MPa; d) −5.0 MPa; e) −7.5 MPa. In each graph, the curves represent different tested pore-fluid pressure values. Theoretical curves based on unrealistic combinations of geological conditions are represented in gray. The *j*/*f* ratios measured in the field for the discussed case studies are plotted with the corresponding uncertainty bars showing an overall good agreement between predicted and measured values. Gray symbols indicate unlikely site conditions as constrained by one or more parameters.

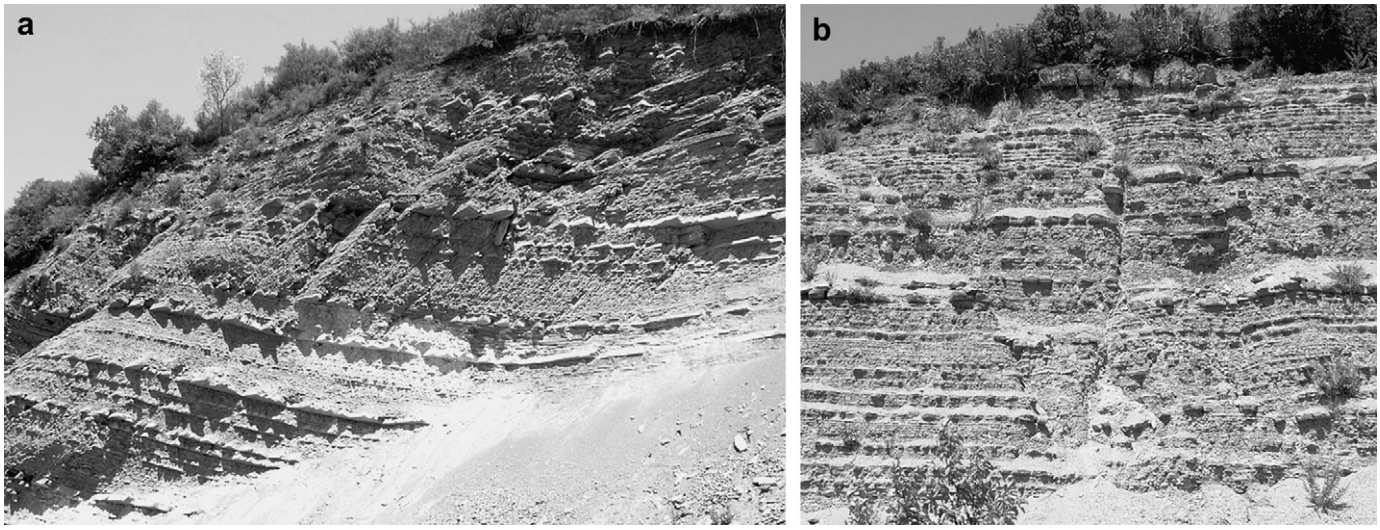

Fig. 4. Examples of layered carbonate fractured rocks: Oligocene–Aquitanian calcarenites alternating with marls (Akarnania, Western Greece). Both cliffs are about 15 m high. Geological, tectonic and stratigraphic settings suggest supra-hydrostatic pore-fluid pressure ($\lambda_e > 0.5$) and at least a moderate strength ($|T_0| > 3$–5 MPa) in agreement with the numerical results (Figs. 3c, d and 4d, e).

than carbonate rocks, Liu et al. (2004) assume $m = 2$ for distributing the elemental seed parameters, like critical strength and Young modulus, within their numerical model. If this value nicely reproduces the heterogeneity within millimetric-scale rock samples, no specific m values have been proposed in the literature for outcrop-scale rock volumes, say a several metres-sided cube. The laboratory problem relative to the size of test samples and the corresponding measured strength value has been investigated so far documenting the general decrease of the mean mechanical properties with increasing sample size (*e.g.* Jaeger and Cook, 1979, and references therein). It is widely accepted that this decrease is due to the increased probability that better oriented and/or better sized flaws are included in a larger specimen (Weibull, 1951). On the other hand, it is also obvious that this variation cannot monotonically persist by further increasing the sample size up to, for example, the outcrop scale. The comparison between large volumes of the same sedimentary succession will likely show a relatively uniform behaviour. Accordingly, at the scale of the modelled unit cell considered in the present paper, corresponding to a cubic portion of a 20–50 cm-thick layer, which represents an intermediate size between the laboratory sample and the outcrop-scale dimensions, a compensation between the tendency of increasing heterogeneity (*i.e.* toward progressively lower m values) and the relative uniformity of large rock volumes (*i.e.* toward higher m values) could be reasonably assumed.

Several values of the heterogeneity index m have been tested during the numerical simulations (2–32). All the results shown in Figs. 2 and 3 are based on $m = 8$, which is likely more appropriate for simulating the behaviour of the regularly layered carbonate rocks considered in this paper (both in numerical modelling and field case studies).

5.5. Geological constraints

The numerical simulations have been carried out by varying the principal parameters in a wide range of values. However, some of the assumed mechanical and geological conditions are indeed very rare in nature. For example, a very low tensile strength (*e.g.* $|T_0| < 1$ MPa), which corresponds to loose or poorly cemented deposits, is possible only at very shallow conditions, say few tens of metres (or a few hundreds, at the most); in contrast, at greater burial depth, where compaction, cementation and diagenetic processes have strongly affected the rock volume, the presence of such weak material is unlikely, if not impossible. This is particularly true for carbonate deposits commonly characterised by a rapid diagenesis and consequent consolidation. Accordingly, the lower shaded areas of Fig. 2 are indicative of a combination of improbable geological and mechanical conditions and hence the calculated j/f ratios falling in this sector of the graph, are likely to be only theoretical.

Following a similar reasoning for the pore-fluid pressure, the numerical simulations have been carried out in a wide range of values, from $\lambda_e = 0$ to $\lambda_e = 0.9$, though at both extreme values some geological constraints are easily found. For example, perfectly dry conditions are only possible in the most superficial rocks and sediments overlying the uppermost aquifer, whereas such hydrogeological conditions are unlikely to occur below few 100 m of overburden. Accordingly, in Fig. 3a, the j/f ratio curves within the shaded area in the right side of the graphs are only theoretical and correspond to unrealistic geological conditions. As for the other pore-fluid pressure end-member ($\lambda_e \gg 0.5$), and considering common geological and tectonic settings where supra-hydrostatic conditions can form and persist during a long lasting deformational event, it is unlikely that such high pore-fluid pressures exist at very shallow depths. There are two major reasons: firstly the burial history would be relatively short and compaction quite limited; secondly, the impermeable cap represented by the overlying deposits would be relatively thin, therefore not sufficient to preserve very high pore-fluid pressures for long time periods. These geologically unrealistic conditions are represented by the shaded areas on the left side of Fig. 3c and d.

6. Comparison with field examples

In order to test the validity and reliability of the conceptual model, the obtained numerical results have been compared with natural case studies of mainly carbonate layered rocks affected by brittle deformation. For each site, several outcrops have been observed to ensure the best possible 3D view together with a precise measurement of the number of joints and faults per unit volume, and hence of their ratio. The fracture counting is averaged from several bedding-parallel views (*i.e.* window sampling) and

variously-oriented sections orthogonal to bedding (*i.e.* scanlines). In order to improve the measured *j*/*f* ratios, a particular care was devoted to recognising the occurrence of crack-jump or crack-seal mechanisms along individual joints/veins. A similar procedure was applied for faults. The range of values represented by the vertical bars in Figs. 2 and 3 considers these uncertainties.

There are three major mechanical and geological parameters that are crucial to determine the *j*/*f* ratio: depth, mean tensile strength, and pore-fluid pressure. Based on i) local and regional geological information, like stratigraphic position and tectonic setting, ii) dedicated field work and/or literature data for each case study, both depth of the burial investigated volumes and pore-fluid pressure have been reasonably inferred. Mean tensile strength has been assessed by comparison between the observed lithologies and similar ones tested in the laboratory. The alternative approach of sampling and laboratory testing of all the investigated rocks has been avoided for the following reasons: firstly, one could not rely on the measured strength because it could be less at the time of the deformational event; secondly, laboratory tests show that carbonate rocks are characterised by a very large variability (*e.g.* Salgado, 2006; Burton et al., 2001; Hoek et al., 2005), which can be better represented by a mean value taken from the literature than by a necessarily limited number of sample values obtained *ad hoc*. Even after such a laboratory effort, the uncertainty on this parameter would have remained. In conclusion, the intrinsic variability of the tensile strength across the whole rock volume has been simulated by using relatively low values of the heterogeneity index (m) of the Weibull distribution function (eq. (2)).

6.1. Akarnania, Greece

The first example is represented by a succession of 10–30 cm-thick relatively well cemented calcarenites alternating with marls (Distraton Fm; IGRS-IFP, 1966; Fig. 4) deposited in the Oligocene–Aquitanian foredeep of the External Hellenides fold-and-thrust belt. The investigated outcrop represents the middle–upper section of the whole stratigraphic sequence and it suffered a possible total burial of about 1.8–2.5 km (IGRS-IFP, 1966). The pore-fluid pressure was probably supra-hydrostatic (*i.e.* $0.6 < \lambda_e < 1$) based on the following considerations: i) the geodynamic setting (a former subsiding basin subsequently affected by thrusting), ii) the lithologies, and iii) the persisting submarine conditions at the time of the deformation (the regional uplift of the area toward sub-aerial exposure occurred later). The investigated rock volume belongs to the outer arc of the Xerovouni anticline, a large-scale fold (IGRS-IFP, 1966); therefore, the tectonic genetic component locally produced tensile stress conditions (*e.g.* Hancock, 1985). The strength of similar marly-siliciclastic flysch lithologies ranges between −1 and −3 to −4 MPa (Christaras, 1997; Dinis da Gama and Navarro Torres, 2002; Hoek et al., 2005). The *j*/*f* ratio averaged from different nearby outcrops is 5×10^3–1×10^4. The site is plotted in Figs. 3c, d and 4c, d in agreement with the *j*/*f* ratio predicted by the numerical model, assuming a tensile strength of at least −3 MPa and a relatively high pore-fluid pressure ($\lambda_e = 0.9$; Fig. 3d). Alternatively, with a lower pore-fluid pressure ($\lambda_e = 0.7$), it would be necessary to assume a slightly higher tensile strength (ca. −8 MPa) as a possible consequence of an advanced lithification process (Fig. 3c). The numerical simulations confirm that a hydrostatic value of the pore-fluid pressure is unrealistic because it would require a much stronger material (ca. −15 MPa; Fig. 3b).

6.2. Somerset, Southern UK

The second field example comes from a sedimentary succession consisting of alternating 10–50 cm-thick beds of fine-grained limestones intercalated with marls (Fig. 5). These Liassic rocks were deposited in a marine environment within the subsiding Bristol Channel basin. Although the tectonic history of the area is polyphased (*e.g.* Rawnsley et al., 1998), the selected site is affected by a set of vertical extension joints striking parallel to a set of normal faults, both of which were likely formed during the Triassic–Aptian rifting phase as documented by synsedimentary tectonic features (Peacock, 2001 and references therein). The maximum overburden at the end of this Early Mesozoic deformational event was 1000–1200 m (Kamerling, 1979), while pore-fluid pressure was supra-hydrostatic (Cosgrove, 2001) because of both a quick burial during subsidence and the low permeability of these deposits. The tensile strength of micritic limestones and marls from laboratory experiments ranges between −1 and −5 MPa (Christaras, 1997; Karakus and Tutmez, 2006). Faults are evenly spaced and the *j*/*f* ratio within 10-m-sided rock volumes varies from infinite (*i.e.* no faults) to ca. 5×10^2, while the ratio averaged at a larger scale is in the range 10^3–10^4. Although there are possible uncertainties in both tensile strength at the time of deformation and/or the degree of supra-hydrostatic conditions, this site (Figs. 3c, d and 4c, d) shows an overall correspondence of the geological estimates and the numerical results. Tensile strengths lower than −7.5 MPa (Fig. 4e), or greater than −1 MPa (Fig. 4b), are unlikely because they would require sub-hydrostatic or close to lithostatic pore-fluid pressure, respectively.

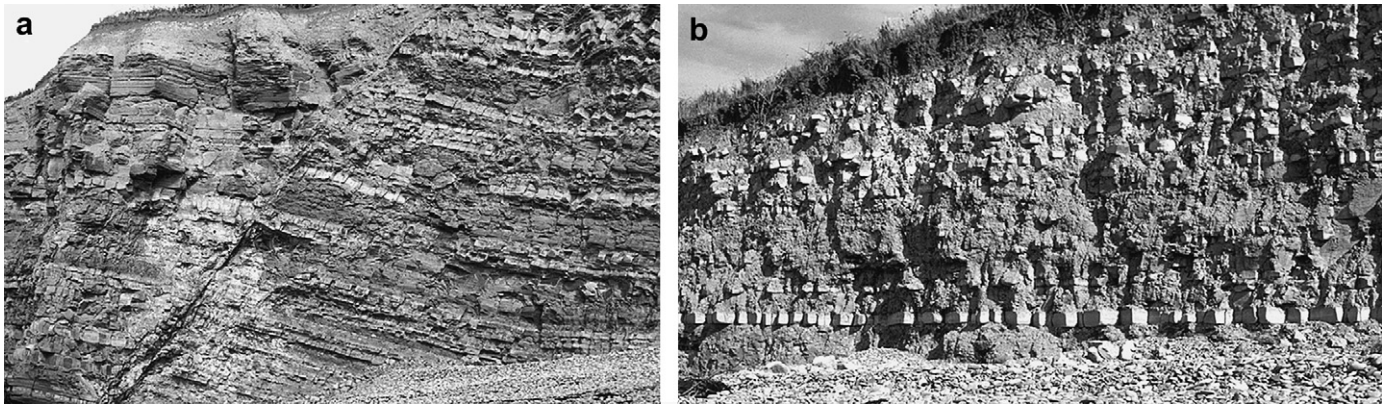

Fig. 5. Examples of layered carbonate fractured rocks: Liassic fine-grained limestones alternating with marls (Somerset, U.K.). The cliffs are 8 (a) and 6 (b) m high. Geological, tectonic and stratigraphic settings suggest supra-hydrostatic pore-fluid pressure ($\lambda_e > 0.5$) and a moderate strength ($|T_0| \sim 2$–5 MPa) in agreement with the numerical results (Figs. 3c, d and 4c, d).

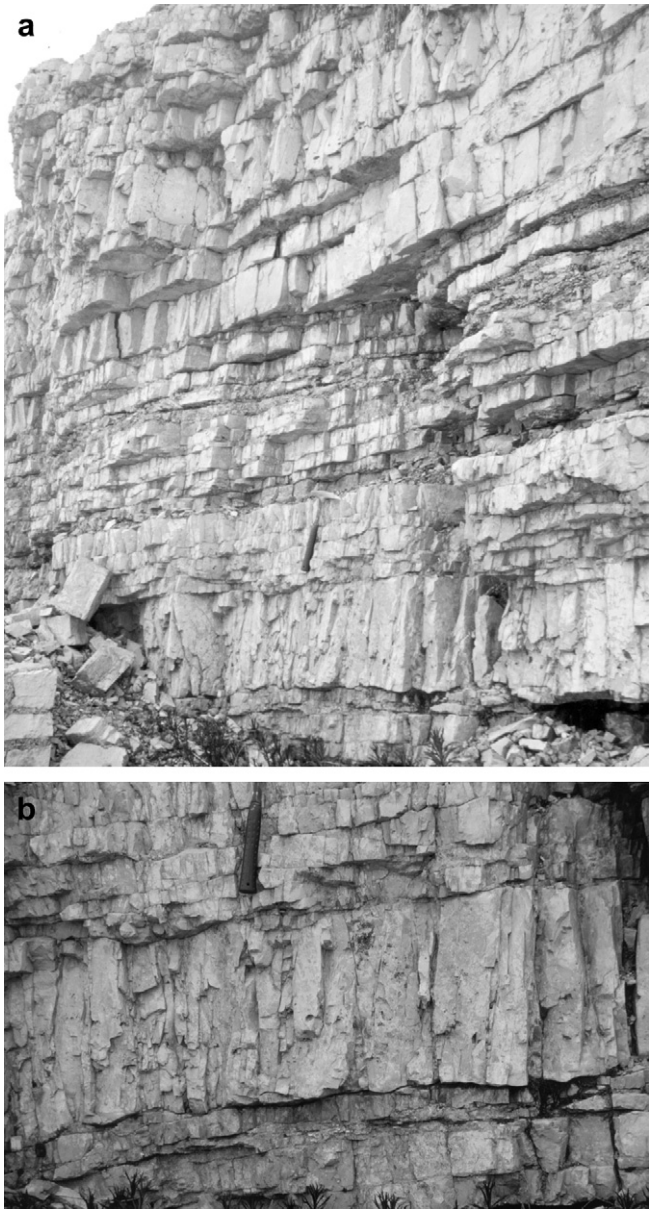

Fig. 6. Examples of layered carbonate fractured rocks: Late Triassic neritic dolostones (Dolomites, Northern Italy). Hammer for scale. Geological, tectonic and stratigraphic settings suggest a hydrostatic to slightly supra-hydrostatic pore-fluid pressure ($\lambda_e \geq 0.4$) and a relatively high strength value ($|T_0| > > 2$–3 MPa) in agreement with the numerical results (Figs. 3b, c and 4d, e).

6.3. Dolomites, Northern Italy

A third field example is represented by a regular cyclic succession of well stratified light brown–white dolomite beds belonging to the Julic (Late Triassic) Heiligkreuz Fm (largely corresponding to the Dürrenstein Fm, *Auctorum*; Fig. 6). In order to constrain the age of the brittle deformational event, the rock volumes selected are those affected by a dense set of extension joints parallel to some major sedimentary dikes that formed during the Rhaetic–Liassic rifting event that affected this sector of Tethys (Winterer and Bosellini, 1981). Based on the thickness of the overlying syntectonic Dolomia Principale, Dachstein and Calcari Grigi Fms (*e.g.* Neri et al., 2007 and references therein), the maximum estimated burial for the investigated case study was 1200–1800 m. These deposits were sedimented in a peri-tidal environment characterised by rapid and mainly sub-contemporaneous lithification and dolomitisation. As a consequence, at the time of the subsequent burial the tensile strength was relatively high since the onset of the deformational event. On the other hand, laboratory tests indicate that the tensile strength for dolostones is generally larger than for limestones and commonly $|T_0| > 5$ MPa (*e.g.* Rossi and Salvi, 2006; Palchik, 2006). Moreover, due to: i) the incipient dolomitisation, ii) the limited compaction during subsequent burial, and iii) the persisting neritic conditions, the pore-fluid pressure remained seemingly close to hydrostatic or slightly supra-hydrostatic. The *j*/*f* ratio estimated from the investigated outcrops is greater than $3–5 \times 10^4$. In Figs. 3b, c and 4d, e, this value nicely fits the above described geological and mechanical conditions. As emphasized in previous examples, the numerical results confirm the above estimates because the alternative assumption of a weak material ($|T_0| < 2$–3 MPa; Fig. 4c) and/or a very high pore-fluid pressure ($\lambda_e = 0.9$; Fig. 3d) was unlikely conditions.

6.4. Salento, Southern Italy

A further case study, but from much shallower conditions, comes from the Salento, Southern Italy. The investigated rocks consist of shallow marine to coastal bioclastic calcarenites of late Early Pleistocene age (Calcareniti di Gravina Fm; Tropeano et al., 2002, and references therein; Fig. 7). The total thickness of this formation locally reaches 150 m. After deposition, the whole area suffered a general uplift accompanied by sedimentation from very limited to absent, and it was affected by a mild though widespread tensile stress field (Di Bucci et al., 2009; Caputo et al., 2008). Since then the carbonate sequence remained under shallow-water or sub-aerial conditions. Accordingly, the pore-fluid pressure was hydrostatic or sub-hydrostatic. Notwithstanding the reduced overburden, the incipient cementation in a sedimentary–diagenetic environment characterised by mixing fresh and salty water was sufficient to produce a relatively stiff material with $|T_0|$ likely close to, or even greater than, 1 MPa (Coviello et al., 2005; Burton et al., 2003; Rossi and Salvi, 2006; Karakus and Tutmez, 2006). In the many surveyed outcrops extensional joints have been widely

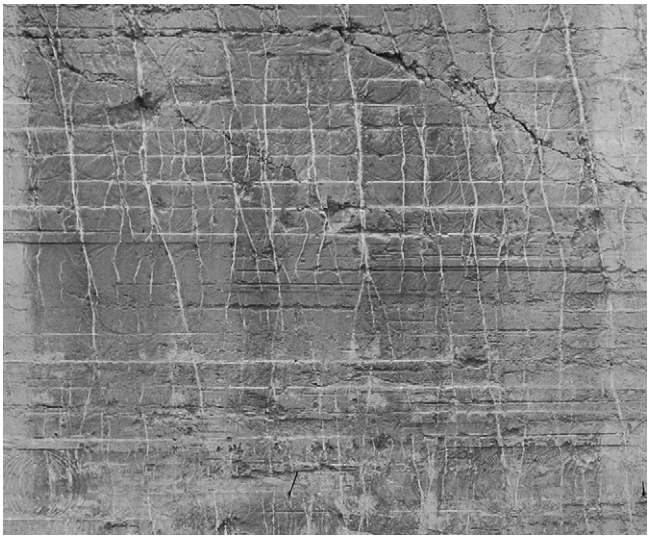

Fig. 7. Examples of layered carbonate fractured rocks: Quaternary marine bioclastic calcarenites (Salento, Southern Italy). The horizontal layering is partly masked by the quarry cuts; the width of the picture is about 5 m (Photo by U. Fracassi). Geological, tectonic and stratigraphic settings suggest a hydrostatic to sub-hydrostatic pore-fluid pressure ($\lambda_e \leq 0.4$) and a low strength value ($|T_0| < 1$–2 MPa) in agreement with the numerical results (Figs. 3a, b and 4b, c).

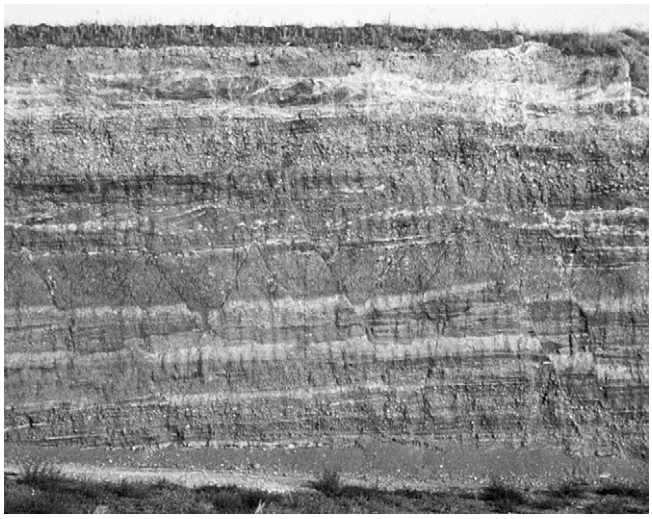

Fig. 8. Examples of layered carbonate fractured rocks: Upper Pliocene–Lower Pleistocene poorly consolidated fluvial sediments (Thessaly, Central Greece). The cliff is about 7 m high. Geological, tectonic and stratigraphic settings suggest a sub-hydrostatic to hydrostatic pore-fluid pressure ($\lambda_e \leq 0.4$) and a very low strength value ($|T_0| << 1$ MPa) in agreement with the numerical results (Figs. 3a, b and 4a).

observed, whereas only a few possible hybrid-shear fractures could be measured. Consequently, the *j*/*f* ratio is very large (10^4–10^5). This site is represented in Figs. 3a, b and 4b, c, fitting the calculated curves with $|T_0| \approx 1$–2 MPa. Indeed, assuming either a weaker ($|T_0| < 0.5$ MPa; Fig. 4a) or a stronger ($|T_0| > 5$ MPa; Fig. 4d) material, the pore-fluid pressure numerically predicted would be supra-hydrostatic or below zero, respectively. Obviously, both cases represent unrealistic geological conditions.

6.5. Thessaly, Central Greece

The last field example (Fig. 8) is from the Pliocene–Lower Pleistocene fluvial sediments cropping out in the Central Hills of Thessaly, Greece (Caputo, 1991). During Middle–Late Quaternary, this area was affected by a uniaxial horizontal tensile stress (Caputo and Pavlides, 1993) and the maximum overburden never exceeded the few tens of metres. Although these deposits are rather more clastic than carbonate, they are interesting because they are characterised by a shallow geological environment (*viz.* a small gravitative genetic component of the stress) similar to the previous case study. However, due to syn- and post-sedimentary conditions, lithology, age and limited overburden, these materials differ from the previous case study because they are poorly consolidated and hence the tensile strength remained very low throughout deformation ($|T_0| < 0.5$ MPa). Like in the previous field example, the pore-fluid pressure was similarly sub-hydrostatic ($\lambda_e \leq 0.4$). In the numerous sections of the quarry, several rupture planes are represented by faults, while relatively few joints occur mainly concentrating in the relatively stiffer argilla-rich layers. Accordingly, the overall *j*/*f* ratio falls within the range 10^0–10^2, therefore fitting the predicted values (Figs. 3a, b and 4a).

7. Concluding remarks

Several mechanical considerations suggest that within a large spectrum of geological and tectonic conditions the fracturing process leads more frequently to the generation of extensional joints than of shear planes (*viz.* faults). Based on the principles of rock mechanics and assuming the most common genetic components of the stress field (Caputo, 2005), a conceptual model is proposed to explain, describe and evaluate this dichotomous behaviour of rocks during a brittle deformational event. Accordingly, using empirical values within commonly accepted ranges for carbonate rocks in shallow crustal conditions for the major mechanical, geological and tectonic parameters, a large number of numerical simulations have been carried out in order to quantify the *j*/*f* ratio. The results of the numerical simulations confirm the predominance of jointing and hence the large *j*/*f* ratios, but they also allow i) to discriminate and evaluate the principal parameters influencing the brittle behaviour of rocks and ii) to decipher the role these parameters play in different geological settings.

The occurrence and distribution of fractures generally control the mechanical properties of rocks like porosity, permeability and strength. Therefore, any realistic prediction pertaining to the fracture pattern and its space and time evolution within a rock mass based on a limited number of data (like in poorly exposed areas or from drillings), is crucial for operators in the oil, water, waste management, mining and rock engineering industries. The proposed model allows prediction of the number of rupturing events and hence their mean ratio. Notwithstanding the well documented coupling between mechanical and diagenetic processes at depth, and hence the tendency for the sub-contemporaneous healing of fractures, the amount of cementation within a newly formed fracture may vary from a total infilling to a limited number of bridges whose size depends on i) time/temperature history of the fracture, which controls precipitation rates and neocrystal volumes, and ii) opening rates (Lander et al., 2002; Laubach et al., 2004a,b). The cement-to-void ratio within fractures could be tentatively inferred together with the secondary permeability of rocks on the basis of diagenetic modelling, burial history and the numerical results of the suggested approach. This represents crucial information for many operators and investigators of the subsoil.

The quantitative estimates should be considered as representative of the mean behaviour of a rock mass. This implies that they are not expected to accurately reproduce the fracture pattern of specific volumes. Unless the most important parameters that influence the mechanical brittle process (like bed thickness, lithology, strength, primary porosity, burial history, nature and thickness of interbedded argilla-rich layers, etc.) and their distribution within a rock mass are perfectly known, such a task will remain utopian.

Although carbonate rocks and carbonate sedimentary successions generally show a relatively large variability, natural field examples representing a variety of geological and tectonic settings and mechanical characteristics have been also considered to test the model. Field measurements of the *j*/*f* ratio in the five case studies are all in agreement with the numerical results obtained by constraining the possible range of values of the most important parameters. It is noteworthy that the numerical simulations can also predict stress conditions favourable to very low *j*/*f* ratios (even <1). However, geological conditions commonly occurring in the upper crustal layers provide important constraints that *de facto* strongly reduce the theoretical possibility of such low ratios and both justify and confirm the reasons why extension joints are generally more abundant than faults in surficial rock volumes that underwent brittle deformational events. Provided the correct parameters are considered, the results and the general discussions of the present paper could be applied to non-carbonate rocks, and in principle, at least as concerns the qualitative aspects of the conceptual model, also to not-layered rocks.

Acknowledgments

Thanks to the Editors of this Special Issue, Fabrizio Agosta and Manuele Tondi, for warmly inviting me to submit a paper on the

topic of the volume. The manuscript has benefited from pleasant discussions with Paul L. Hancock many years ago and from constructive comments on an early draft by Daniela Di Bucci. Critical reading by anonymous reviewers, the guest-editors and Tom Blenkinsop also contributed to improve the text.

References

Al-Shayea, N., 2002. Comparison of fracture toughness behavior of reservoir and outcrop specimens from a limestone rock formation tested at various conditions. J. Rock Mech. Rock Eng. 35 (4), 271–297.

Atkinson, B.K. (Ed.), 1987. Fracture Mechanics of Rock. Academic Press, London, p. 534.

Austin, N.J., Kennedy, L.A., 2005. Textural controls on the brittle deformation of dolomite: variations in peak strength. In: Gapai, D., Brun, J.P., Cobbold, P.R. (Eds.), Deformation Mechanisms, Rheology and Tectonics: from Minerals to the Lithosphere. Geological Society, London, Special Publications, vol. 243, pp. 37–49.

Backers, T., 2004. Fracture Toughness Determination and Micromechanics of Rock Under Mode I and Mode II Loading. Ph.D. thesis. Potsdam University, p. 137, http://deposit.ddb.de/cgi-bin/dokserv?idn=974306118&dok_var=d1&dok_ext=pdf&filename=974306118.pdf.

Bai, T., Pollard, D.D., 2000. Fracture spacing in layered rocks: a new explanation based on the stress transition. J. Struct. Geol. 22, 43–57.

Bai, T., Maerten, L., Gross, M.R., Aydin, A., 2002. Orthogonal cross joints: do they imply a regional stress rotation? J. Struct. Geol. 24, 77–88.

Barker, C., 1972. Aquathermal pressuring: role of temperature in development of abnormal pressure zone. Am. Assoc. Pet. Geol. Bull. 56, 2068–2071.

Brace, W.F., 1964. Brittle fracture of rocks. In: Judd, W.R. (Ed.), State of Stress in the Earth's Crust. Elsevier, New York, pp. 111–174.

Burton, C.L., Waltham, A.C., McLaren, S.J., 2001. Strength variation in young reef limestones. Géotechnique 51 (10), 887–889.

Burton, C.L., Waltham, A.C., McLaren, S.J., 2003. Strength variation in young reef limestones. Géotechnique 53 (8), 764–766.

Caputo, M., Caputo, R., 1989. Estimate of the regional stress field using joint systems. Bull. Geol. Soc. Greece XXIII (1), 101–118.

Caputo, R., 1991. A comparison between joints and faults as brittle structures used for evaluating the stress field. Ann. Tectonicae 5 (1), 74–84.

Caputo, R., 1995. Evolution of orthogonal sets of coeval extension joints. Terra Nova 7 (5), 479–490.

Caputo, R., 2001. Why are extension joints more abundant than faults? In: Paul L. Hancock Memorial Meeting on Mechanisms of Jointing in the Crust, Weston Super Mare, U.K., August 1–4, 2001, abstracts, pp. 42–43.

Caputo, R., 2005. Stress variability and brittle tectonic structures. Earth Sci. Rev. 70 (1–2), 103–127.

Caputo, R., Hancock, P.L., 1999. Crack-jump mechanism of microvein formation and its implications for stress cyclicity during extension fracturing. J. Geodyn. 27, 45–60. Oxford.

Caputo, R., Pavlides, S., 1993. Late Cainozoic geodynamic evolution of Thessaly and surroundings (Central–Northern Greece). Tectonophysics 223 (3–4), 339–362.

Caputo, R., Di Bucci, D., Mastronuzzi, G., Fracassi, U., Selleri, G., Sansò, P., 2008. Late Quaternary extension of the southern Adriatic foreland (Italy): evidence from joint analysis. Rend. Online Soc. Geol. It. 1, 62–67.

Carmichael, R.S. (Ed.), 1982, Practical Handbook of Physical Properties of Rocks, vol. II. CRC Press, Boca Raton, Fla, p. 273.

Chang, C., Zoback, M.D., Khaksar, A., 2006. Empirical relations between rock strength and physical properties in sedimentary rocks. J. Pet. Sci. Eng. 51, 223–237.

Chapple, W.M., 1969. Fold shape and rheology: the folding of an isolated, viscous-plastic layer. Tectonophysics 7 (2), 97–116.

Christaras, B., 1997. Landslides in iliolitic and marly formations. Examples from north-western Greece. Eng. Geol. 47, 57–69.

Cosgrove, J.W., 2001. Hydraulic fracturing during the formation and deformation of a basin: a factor in the dewatering of low-permeability sediments. Am. Assoc. Pet. Geol. Bull. 85 (4), 737–748.

Coviello, A., Lagioia, R., Nova, R., 2005. On the measurement of the tensile strength of soft rocks. J. Rock Mech. Rock Eng. 38 (4), 251–273.

Curtis, R.V., Juszczyk, A.S., 1998. Analysis of strength data using two- and three-parameter Weibull models. J. Mater. Sci. 33, 1151–1157.

Davies, I.J., 2001. Empirical correction factor for the best estimate of Weibull modulus obtained using linear least square analysis. J. Mater. Sci. Lett. 20, 997–999.

Di Bucci, D., Coccia, S., Fracassi, U., Iurilli, V., Mastronuzzi, G., Palmentola, G., Mastronuzzi, G., Sansò, P., Selleri, G., Valensise, G., 2009. Late Quaternary deformation of the southern Adriatic foreland (southern Apulia) from meso-structural data: preliminary results. J. Geosci. (Boll. Soc. Geol. It.) 128 (1), 33–46.

Dickinson, G., 1953. Geological aspects of abnormal reservoir pressures in Gulf Coast Louisiana. Am. Assoc. Pet. Geol. Bull. 37, 410–432.

Dinis da Gama, C., Navarro Torres, V., 2002. Prediction of EDZ (excavation damaged zone) from explosive detonation in underground openings. In: Proceedings of ISRM-Eurock 2002, Funchal, November 25–28, 2002.

Dunne, W.N., Hancock, P.L., 1994. Palaeostress analysis of small-scale brittle structures. In: Hancock, P.L. (Ed.), Continental Deformation. Pergamon Press, Oxford, pp. 101–120.

Engelder, T., 1999. Transitional-tensile fracture propagation: a status report. J. Struct. Geol. 21, 1049–1055.

Engelder, T., Fischer, M.P., Gross, M.R., 1993. Geological aspects of fracture mechanics. In: Geological Society of America, Short Course Manual, p. 281.

Etheridge, M.A., 1983. Differential stress magnitudes during regional deformation and metamorphism: upper bound imposed by tensile fracturing. Geology 11, 231–234.

Fairhurst, C., 1961. Laboratory measurement of some physical properties of rock. In: Proceedings of the Fourth Symposium Rock Mechanics. Penn. State University, pp. 105–118.

Fertl, W.H., Chapman, R.E., Hotz, R.F. (Eds.), 1994. Studies in Abnormal Pressures. Developments in Petroleum Science. Elsevier, New York, p. 472.

Fookes, P.G., Higginbottom, I.E., 1975. The classification and description of near-shore carbonate sediments for engineering purposes. Géotechnique 25 (2), 406–411.

Fyfe, W.S., Price, N.J., Thompson, A.B., 1978. Fluids in the Earth's Crust. Elsevier, New York.

Gale, F.W., Laubach, S.E., Marrett, R.A., Olson, J.E., Holder, J., Reed, R.M., 2004. Predicting and characterizing fractures in dolostone reservoirs: using the link between diagenesis and fracturing. In: Braithwaite, C.J.R., Rizzi, G., Darke, G. (Eds.), The Geometry and Petrogenesis of Dolomite Hydrocarbon Reservoirs. Geological Society, London, Special Publications, vol. 235, pp. 177–192.

Gillespie, P.A., Walsh, J.J., Watterson, J., Bonson, C.G., Manzocchi, T., 2001. Scaling relationships of joint and vein arrays from The Burren Co. Clare, Ireland. J. Struct. Geol. 23, 183–201.

Gross, M.R., 1993. The origin and spacing of cross joints: examples from the Monterey Formation, Santa Barbara Coastline, California. J. Struct. Geol. 15 (6), 737–751.

Hancock, P.L., 1985. Brittle microtectonics: principles and practice. J. Struct. Geol. 7, 437–457.

Hancock, P.L., Al-Kadhi, A., Barka, A.A., Bevan, T.G., 1987. Aspects of analysing brittle structures. Ann. Tectonicae 1 (1), 5–19.

Harris, J.F., Taylor, G.L., Walper, J.L., 1960. Relation of deformation fractures in sedimentary rocks to regional and local structures. Am. Assoc. Pet. Geol. Bull. 44, 1853–1873.

Harrison, W.J., Summa, L.L., 1991. Paleohydrology of the Gulf of Mexico Basin. Am. J. Sci. 291, 109–176.

Hobbs, D.W., 1967. The formation of tension joints in sedimentary rocks: an explanation. Geol. Mag. 104, 550–556.

Hoek, E., Marinos, P.G., Marinos, V.P., 2005. Characterisation and engineering properties of tectonically undisturbed but lithologically varied sedimentary rock masses. Int. J. Rock Mech. Min. Sci. 42, 277–285.

I.G.R.S.-I.F.P., 1966. Etude géologique de l'Epire. In: Technip (Ed.), Paris, 306 pp.

Ingraffea, A.R., 1987. Theory of crack initiation and propagation in rock. In: Atkinson, B.K. (Ed.), Fracture Mechanics of Rock. Academic Press, pp. 71–110.

Jaeger, J.C., Cook, N.G.W., 1979. Fundamentals of Rock Mechanics. Chapman and Hall, London.

Jaeger, J.C., Hoskins, E.R., 1966. Stresses and failure in rings of rock loaded in diametral tension or compression. Br. J. Appl. Phys. 17, 685–692.

Kamerling, P., 1979. The geology and hydrocarbon habitat of the Bristol Channel Basin. J. Pet. Geol. 2, 75–93.

Karakus, M., Tutmez, B., 2006. Fuzzy and multiple regression modelling for the evaluation of intact rock strength based on point load, Schmidt hammer and sonic velocity. J. Rock Mech. Rock Eng. 39 (1), 45–57.

Ladeira, F.L., Price, N.J., 1981. Relationship between fracture spacing and bed thickness. J. Struct. Geol. 3 (2), 179–183.

Lama, R.D., Vutukuri, V.S., 1978. Handbook on Mechanical Properties of Rocks, vol. II. Trans Tech Publications, Clausthal, Germany.

Lander, R.H., Gale, J.F.W., Laubach, S.E., Bonnell, L.M., 2002. Interaction between quartz cementation and fracturing in sandstones. Am. Assoc. Pet. Geol. Bull. Annual Convention, Abstracts, 11 (CD).

Laubach, S.E., Reed, R.M., Olson, J.E., Lander, R.H., Bonnell, L.M., 2004a. Coevolution of crack-seal texture and fracture porosity in sedimentary rocks: cathodoluminescence observations of regional fractures. J. Struct. Geol. 26, 967–982.

Laubach, S.E., Lander, R.H., Bonnell, L.M., Olson, J.E., Reed, R.M., 2004b. Opening histories of fractures in sandstones. In: Cosgrove, J.W., Engelder, T. (Eds.), The Initiation, Propagation, and Arrest of Joints and Other Fractures. Geological Society, London, Special Publications, vol. 231, pp. 1–9.

Liu, H.Y., Roquete, M., Kou, S.Q., Lindqvist, P.-A., 2004. Characterization of rock heterogeneity and numerical verification. Eng. Geol. 72, 89–119. doi:10.1016/j.enggeo.2003.06.004.

Magara, K., 1975. Re-evaluation of montmorillonite dehydration as cause of abnormal pressure and hydrocarbon migration. Am. Assoc. Pet. Geol. Bull. 59, 292–302.

Mouchet, J.P., Mitchell, A., 1989. Abnormal Pressures While Drilling. In: Manuels techniques elf aquitaine, vol. 2. Elf Aquitaine, Boussens, France.

Murrell, S.A.F., 1963. A criterion for brittle fracture of rocks and concrete under triaxial stress and the effect of pore pressure on the criterion. In: Fairhurst, C. (Ed.), Proceedings of the Fifth Rock Mechanics Symposium on Rock Mechanics. University of Minnesota, Pergamon, Oxford, pp. 563–577.

Narr, W., Burruss, R.C., 1984. Origin of reservoir fractures in Little Knife Field, North Dakota. Am. Assoc. Pet. Geol. Bull. 68 (9), 1087–1100.

Narr, W., Currie, J.B., 1982. Origin of fracture porosity – example from Altamont Field, Utah. Am. Assoc. Pet. Geol. Bull. 66 (9), 1231–1247.

Neri, C., Gianolla, P., Furlanis, S., Caputo, R., Bosellini, A., 2007. Note Illustrative della Carta Geologica d'Italia alla scala 1:50.000, foglio 029 Cortina d'Ampezzo. APAT, Roma, p. 200.

Nicol, A., Watterson, J., Walsh, J.J., Childs, C., 1996. The shapes, major axis orientations and displacement patterns of fault surfaces. J. Struct. Geol. 18 (2–3), 235–248.

Nur, A., 1982. The origin of tensile fracture lineaments. J. Struct. Geol. 4 (1), 31–40.
Palchik, V., 2006. Stress–strain model for carbonate rocks based on Haldane's distribution function. J. Rock Mech. Rock Eng. 39 (3), 215–232.
Peacock, D.C.P., 2001. The temporal relationship between joints and faults. J. Struct. Geol. 23, 329–341.
Peacock, D.C.P., 2002. Propagation, interaction and linkage in normal fault systems. Earth Sci. Rev. 58, 121–142.
Peacock, D.C.P., 2004. Differences between veins and joints using the example of the Jurassic limestones of Somerset. In: Cosgrove, J.W., Engelder, T. (Eds.), The Initiation, Propagation, and Arrest of Joints and Other Fractures. Geological Society, London, Special Publications, vol. 231, pp. 209–221.
Peacock, D.C.P., Sanderson, D.J., 1991. Displacement, segment linkage and relay ramps in normal fault zones. J. Struct. Geol. 13, 721–733.
Pollard, D.D., Aydin, A., 1988. Progress in understanding jointing over the past century. Geol. Soc. Am. Bull. 100, 1181–1204.
Pollard, D.D., Segall, P., 1987. Theoretical displacements and stresses near fractures in rock: with applications to faults, joints, veins, dikes, and solution surfaces. In: Atkinson, B.K. (Ed.), Fracture Mechanics of Rocks. Academic Press, pp. 277–349.
Powers, M.C., 1967. Fluid-release mechanisms in compacting marine mudrocks and their importance in oil exploration. Am. Assoc. Pet. Geol. Bull. 51, 1240–1245.
Price, N., 1966. Fault and Joint Development in Brittle and Semi-Brittle Rock. Pergamon Press, Oxford, 176 pp.
Price, N.J., Cosgrove, J.W., 1990. Analysis of Geological Structures. Cambridge University Press, Cambridge, 502 pp.
Ramsay, J.G., 1980. The crack-seal mechanism of rock deformation. Nature 284, 135–139.
Rawnsley, K.D., Peacock, D.C.P., Rives, T., Petit, J.-P., 1998. Joints in the Mesozoic sediments around the Bristol Channel Basin. J. Struct. Geol. 20 (12), 1641–1661.
Renard, F., Park, A., Ortoleva, P., Gratier, J.-P., 1999. An integrated model for transitional pressure solution in sandstone. Tectonophysics 312, 97–115.
Roberts, J.C., 1974. Jointing and minor tectonics of the Vale of Glamorgan between Ogmore-by-Sea and Lavernock Point, South Wales. Geol. J. 9 (2), 97–114.
Rossi, F., Salvi, F., 2006. In: Zanichelli/ESAC (Ed.)Manuale di Ingegneria Civile, third ed., vol. 1, Bologna, p. 1312.
Salgado, R., 2006. The Engineering of Foundations. McGraw-Hill, Boston, p. 896.
Secor, D.T., 1965. Role of fluid pressure in jointing. Am. J. Sci. 263, 633–646.
Terzaghi, K., 1943. Theoretical Soil Mechanics. J. Wiley & Sons, New York.
Tropeano, M., Sabato, L., Pieri, P., 2002. Filling and cannibalization of a foredeep: the Bradanic Trough (Southern Italy). In: Jones, S.J., Frostick, L.E. (Eds.), Sediment Flux to Basins: Causes, Controls and Consequences. Geological Society, London, Special Publications, vol. 191, pp. 55–79.
Tuncay, K., Park, A., Ortoleva, P., 2000. Sedimentary basin deformation: an incremental stress approach. Tectonophysics 323, 77–104.
Weibull, W., 1939. A statistical theory of the strength of materials. In: Ingvetensk. Akad. Handl., No. 151.
Weibull, W., 1951. A statistical distribution function of wide applicability. J. Appl. Mech. 18, 293–297.
Winterer, E.L., Bosellini, A., 1981. Subsidence and sedimentation on Jurassic passive continental margin, Southern Alps, Italy. Am. Assoc. Pet. Geol. Bull. 65, 394–421.
Zhang, Z.X., 2002. An empirical relation between mode I fracture toughness and the tensile strength of rock. Int. J. Rock Mech. Min. Sci. 39, 401–406.
Zoback, M.D., Zoback, M.L., 1991. Tectonic stress field on North America and relative plate motions. In: Slemmons, D.B., Engdahl, E.R., Zoback, M.D., Blackwekk, D.D. (Eds.), The Geology of North America, Decade Map. Neotectonics of North America, vol. 1. Geologcial Society of America, Boulder, Colorado, pp. 339–366.